Global Biogeochemical Cycles

RESEARCH ARTICLE
10.1029/2018GB006135

Underestimation of Global Photosynthesis in Earth System Models Due to Representation of Vegetation Structure

R. K. Braghiere[1,2,3,4], T. Quaife[4], E. Black[5], L. He[6,7], and J. M. Chen[6]

[1]Jet Propulsion Laboratory, California Institute of Technology, Pasadena, CA, USA, [2]Joint Institute for Regional Earth System Science and Engineering, University of California, Los Angeles, CA, USA, [3]INRA-Supagro, Montpellier, France, [4]National Centre for Earth Observation, Department of Meteorology, University of Reading, Reading, UK, [5]National Centre for Atmospheric Science, Department of Meteorology, University of Reading, Reading, UK, [6]Department of Geography and Program in Planning, University of Toronto, Toronto, Ontario, Canada, [7]Laboratory of Environmental Model and Data Optima, Laurel, MD, USA

Key Points:
- Earth System Models (ESMs) may significantly underestimate global photosynthesis because they do not take vegetation structure into account
- Introducing vegetation clumping into ESMs with multilayered canopy schemes alleviates light limitation of photosynthesis at lower canopy levels
- In our study, the addition of vegetation clumping into the land surface scheme of the UKESM resulted in an additional uptake of carbon by photosynthesis of 5.53 PgC/year globally and 4.18 PgC/year between 20°S and 20°N latitude

Correspondence to:
R. K. Braghiere,
renato.braghiere@gmail.com

Citation:
Braghiere, R. K., Quaife, T., Black, E., He, L., & Chen, J. M. (2019). Underestimation of global photosynthesis in Earth System Models due to representation of vegetation structure. *Global Biogeochemical Cycles*, *33*, 1358–1369. https://doi.org/10.1029/2018GB006135

Received 16 NOV 2018
Accepted 15 SEP 2019
Accepted article online 11 OCT 2019
Published online 8 NOV 2019

Abstract The impact of vegetation structure on the absorption of shortwave radiation in Earth System Models (ESMs) is potentially important for accurate modeling of the carbon cycle and hence climate projections. A proportion of incident shortwave radiation is used by plants to photosynthesize and canopy structure has a direct impact on the fraction of this radiation which is absorbed. This paper evaluates how modeled carbon assimilation of the terrestrial biosphere is impacted when clumping derived from satellite data is incorporated. We evaluated impacts of clumping on photosynthesis using the Joint UK Land Environment Simulator, the land surface scheme of the UK Earth System Model. At the global level, Gross Primary Productivity (GPP) increased by 5.53 ± 1.02 PgC/year with the strongest absolute increase in the tropics. This is contrary to previous studies that have shown a decrease in photosynthesis when similar clumping data sets have been used to modify light interception in models. In our study additional transmission of light through upper canopy layers leads to enhanced absorption in lower layers in which photosynthesis tends to be light limited. We show that this result is related to the complexity of canopy scheme being used.

Plain Language Summary Plants need sunlight to photosynthesize; however, the way in which light absorption is typically described by climate models is not very realistic because it does not take into account structural differences in forest canopies. Identifying more realistic ways to represent these processes in forests would allow us to better predict photosynthesis and to have a greater understanding of the impact of future climate change. In our paper we discuss a method to include information about vegetation structure derived from satellites in climate models. Our results indicate that such models underestimate the amount of light reaching plants in the lower layers of dense forests. Consequently, global photosynthesis is likely underestimated in climate models due to a lack of consideration of plant structural variability.

1. Introduction

Understanding the global carbon cycle is critically important for understanding current and future climate change. The terrestrial biosphere sequesters around 25% of anthropogenic carbon emissions (Le Quéré, Andrew, Friedlingstein, Sitch, Hauck, et al., 2018) but there remains uncertainty around exactly what processes drive this (Ciais et al., 2019) and whether or not this sink will be maintained in the future. A reduction in sink strength due to climatic factors could be a significant positive feedback to climate change. To be able to model the future evolution of this uptake of carbon requires the ability to correctly model the underlying processes. This paper focuses specifically on photosynthesis in the terrestrial biosphere and the how we model the light interception in plants which drives this.

The uptake of carbon by terrestrial photosynthesis is the largest component flux in the global carbon cycle. Despite this its overall magnitude and global spatial distribution remains poorly understood. Estimates of Gross Primary Productivity (GPP) in the literature range from 120 to 175 PgC/year. The estimate of global GPP presented in the first IPCC report was set in the interval 90–120 PgC/year (Watson et al., 1990) followed by all the other IPCC reports giving a fixed global GPP value equals to 120 PgC/year (Denman et al., 2007;

Melillo et al., 1995; Prentice et al., 2001). More recently, the last IPCC report (Ciais et al., 2013) updated the value of global GPP to 123 ± 8 PgC/year based on model tree ensemble (MTE) and Eddy Covariance (EC) flux (Beer et al., 2010); however, the value of GPP strongly depends on the method used and they often disagree in long-term trends and spatial patterns (Anav et al., 2015; He, Chen, Liu, et al., 2017; He, Chen, Croft, et al., 2017; Jiang & Ryu, 2016; Jung et al., 2011; Knauer et al., 2017; MacBean et al., 2018).

For the global carbon budget 2007–2016, an imbalance of 0.6 PgC/year was estimated, indicating possible underestimated values in carbon sinks, such as global photosynthesis (Le Quéré Andrew, Friedlingstein, Sitch, Pongratz, et al., 2018). Welp et al. (2011) estimated global GPP to be somewhere in between 150 and 175 PgC/year based on $^{18}O/^{16}O$, and in a study based on ^{13}C it was found that more GPP should be attributed to the Amazon region (Chen et al., 2017). Koffi et al. (2012) presented a study based on data assimilation with atmospheric CO_2 and ecosystem models with an estimated global GPP of 146 ± 19 PgC/year. More recent studies using Solar Induced Florescence (SIF) predicted global GPP to be 144 PgC/year; closer to most Earth System Models (ESMs) estimates than the MTE or MODIS data sets (Anav et al., 2015).

A key process required for modeling photosynthesis is the interception of light, which is typically achieved using a vegetation radiative transfer (RT) model. A commonly used vegetation RT model in many ESMs is the two-stream scheme of Sellers (1985) and a key assumption in the Sellers scheme is that leaves are randomly arranged in a plane parallel medium. This assumption is in common with many other vegetation RT schemes and is almost ubiquitous among those used in Climate and Earth System models. In reality, however, vegetation does not arrange itself in such a perfectly random fashion. An important question, therefore, is to ask what extent this assumption affects predictions of the photosynthetic flux of carbon into the land surface.

A simplification that results from the plane-parallel turbid medium approximation is a lack of representation of gaps in the canopies. The term "gaps" is used here in the sense of "openness," that is, canopy openings, which light goes through without being intercepted. For most natural forest stands, savannah, and shrubland, various sizes of gaps exist between and within tree crowns. Neglecting these gaps has been shown to result in errors when estimating shortwave radiation interception.

Previous studies have shown that two-stream schemes can exhibit significant biases in comparison to more accurate three-dimensional (3-D) radiative transfer models and observations (Pinty et al., 2006; Ni-Meister et al., 2010; Kobayashi et al., 2012; Loew et al., 2014; Hogan et al., 2018). Despite this two-stream schemes remain attractive due to their computational efficiency. Highly detailed 3-D radiative transfer models exist but they cannot be directly used in ESMs due to their computational expense (Yang et al., 2001) and the large number of parameters required (Loew et al., 2014). One approach to account for 3-D canopy structure in two-stream schemes is to include simple parameterizations of 3-D effects on shortwave radiation partitioning (Pinty et al., 2006). In the present study, we modify JULES, the land surface scheme of the UK Earth System Model (UKESM), to ingest a global data set of canopy clumping derived from satellite data, in order to determine the impact of vegetation canopy structure on modeled global photosynthesis. Although this modification results less light absorption by vegetation in the model it also drives an additional uptake of carbon by photosynthesis of 5.53 PgC/year globally and 4.18 PgC/year between 20°S and 20°N latitude. The primary mechanism we attribute this to is the increased amount of light reaching lower layers of the canopy in which photosynthesis tends to be limited by available light. Conversely, photosynthesis in the upper canopy layers, which absorb less light once clumping is included, are not typically light limited and so the reduction in absorbed radiation has less impact.

2. Models and Methods

2.1. Model Description

The most commonly used method to account for structure in a vegetation RT model is to introduce a clumping index (Ω) (Nilson, 1971) to scale leaf area index (LAI). This can be easily implemented into the two-stream scheme; wherever LAI appears in the equations it is scaled by Ω. Hence, the two stream equations become

$$\overline{\mu}\frac{(dI^{\uparrow})}{dLAI}+[1-[1-\beta]\omega]I^{\uparrow}-\omega\beta I^{\downarrow}=\omega\overline{\mu}\beta_0\exp(-KL\cdot\Omega),\overline{\mu}\frac{(dI^{\downarrow})}{dLAI}+[1-[1-\beta]\omega]I^{\downarrow}-\omega\beta I^{\uparrow}$$
$$=\omega\overline{\mu}(1-\beta_0)\exp(-KL\cdot\Omega) \quad (1)$$

where $I^{\uparrow}$ and $I^{\downarrow}$ are the upward and downward diffuse radiative fluxes normalised by the incident flux at the top of the canopy; μ is the cosine of the Sun zenith angle, or the incident beam; K is the optical depth of direct beam per unit leaf area and is equal to $G(\mu)/\mu$, where $G(\mu)$ is the projected area of leaf elements in the direction $\cos^{-1}\mu$ (Ross, 1981); $\overline{\mu}$ is the average inverse diffuse optical depth per unit leaf area; ω is the scattering coefficient and is given by $\rho_{leaf}+\tau_{leaf}$, the leaf reflectance and transmittance, respectively; and L is the cumulative LAI from the top of the canopy. β and β_0 are upscattering parameters for the diffuse and direct beams, respectively. In this context Ω corresponds to the structure factor described in Pinty et al. (2006) except that it is assumed not to vary with zenith angle.

The Joint UK Land Environment Simulator (JULES; Best et al., 2011; Clark et al., 2011) is the land surface scheme of the new UK Earth System Model (UKESM). It uses the Sellers RT model to calculate light interception and absorption in vegetation. The option to include a clumping index was added in version 4.6 with a default value of 1.0 (i.e., no clumping), allowing user to prescribe other values where data are available. The variable was originally implemented in JULES with a single value per plant functional type (PFT), and it was tested and evaluated over crops by Williams et al. (2017), who showed that it was necessary to include clumping (i.e., $\Omega < 1.0$) to correctly model the productivity of maize for a field site in Nebraska, USA. For this paper we modified JULES to read in a spatially varying map of clumping for each PFT (described in section 2.2).

We used JULES version 4.6 with the Global Land (GL) 4.0 configuration (Walters et al., 2014) with the WATCH-Forcing-Data-ERA-Interim data set (Weedon et al., 2014) at 0.5° spatial resolution and temporal resolution of 3 hr. The Harmonized World Soil Database version 1.0 data set (Nachtergaele et al., 2008) and the model of runoff production (TOPMODEL) were applied following Clark and Gedney (2008). Leaf area index was determined prognostically by the JULES phenology module (Cox, 2001) updated every 10 days. Prior to performing the global scale model simulations, the soil moisture and temperature were brought to equilibrium using a five-year global spin-up by cycling one year of meteorological data. JULES GL4.0 uses five PFTs: broadleaf trees, needle-leaf tress, C3 grasses, C4 grasses, and shrubs.

By default, JULES computes light interception and photosynthesis in 10 vertical canopy layers. Leaf-level photosynthesis in each layer is estimated as the minimum rate of three assimilation regimes as proposed by Farquhar et al. (1980) and modified by Collatz et al. (1991) and Collatz et al. (1992): (i) the Rubisco-limited rate or carbon limiting regime, (ii) the light-limited rate, and (iii) the carbon compound export limitation for C3 plants or PEP-carboxylase export limitation for C4 plants, referred to as the electron transport or export limiting regime. The multilayer approach simulates the transition between the Farquhar limiting regimes at each canopy layer, resulting in increased carbon limitation toward the top of the canopy and increased light limitation toward the bottom of the canopy (Clark et al., 2011). The light-limited rate of photosynthesis in each layer is proportional to the fraction of absorbed photosynthetically active radiation (fAPAR) in that layer. Consequently, including clumping in the radiative transfer scheme directly affects the light-limited rate of photosynthesis but not the Rubisco or export-limited rates.

We performed two runs of JULES for the year 2008 with and without a prescribed value of clumping index. The year was chosen as it is close to the date of production of the clumping map (i.e., 2006) and an ENSO neutral year, unlike 2006–2007, which was a weak El Niño.

2.2. Global Clumping Index Map

The global clumping map of He et al. (2012) was used to provide clumping index data for JULES. It has a spatial resolution of 500 m and was produced for the year of 2006. We assume that the global clumping index map in 2006 is still reliable for modeling GPP in 2008 since the interannual variation of clumping index is generally small (He et al., 2016). The data were derived from the NASA-MODIS BRDF/albedo product (MCD43) by considering the difference in forward and backward scattering from the surface, which is primarily controlled by the structure of the vegetation. This follows the methodology of Chen and Leblanc (2005) but with an additional correction to the magnitude of the MODIS hot spot. The method uses a

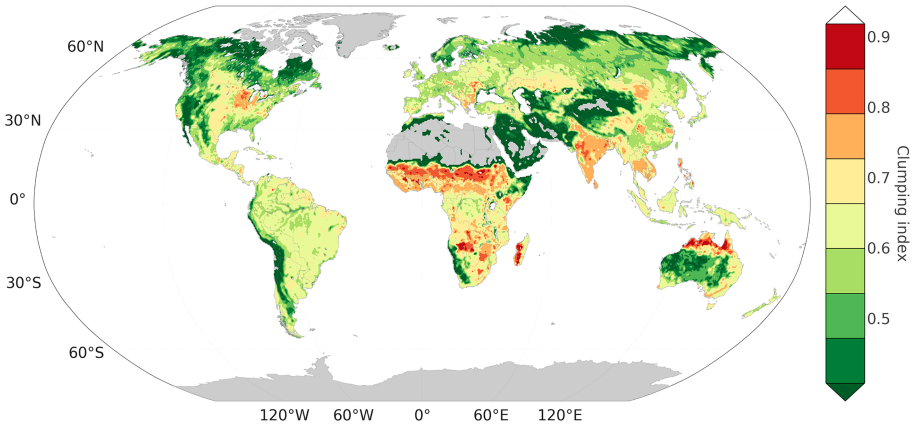

Figure 1. Global map of the MODIS derived clumping index at 0.5° resolution for the year 2006 scaled up from the 500 m He et al. (2012) clumping data set.

four-Scale BRDF model (Chen & Leblanc, 1997) that considers different scales of canopy clumping: tree groups, tree crowns, branches, and shoots. This is equivalent to the assumptions implicit in clumping as implemented in JULES. Pinty et al. (2006) provide a detailed discussion of this type of clumping index as applied to two-stream models.

We scaled up the He et al. (2012) data to the resolution of the model run (0.5°) on a per-PFT basis by using the GLC2000 land cover data (Bartholomé & Belward, 2005). The GLC2000 is also used in the production of the clumping data set and to prescribe the distribution of the five PFTs used by JULES. The total clumping index map is shown in Figure 1. Values less than 1 indicate clumping, with smaller values indicating greater clumping. The most clumped areas are the boreal forests and areas with sparse vegetation, while the least clumped areas are in the presence of grasses, that is, over savannahs in Africa and crops in the USA and Asia. Tropical forests show intermediate levels of clumping, which does not fit with many below canopy observations of clumping. He et al. (2012) argue that ground-based measurements generally underestimate clumping in dense forests (i.e., overestimate the clumping index value) because they are overly affected by lower level branches. Pisek and Oliphant (2013) further confirmed that in moderate to dense forests with developed bottom layers, in situ measurements of clumping near the surface tend to considerably underestimate the overall canopy-level clumping. Olivas et al. (2013) found that the mean LAI above 1 m using litterfall collection was 5.54 $\pm$ 0.30 at an old-growth tropical rainforest, while the effective LAI from hemispherical photographs was only 3.45 $\pm$ 0.10, implying a clumping index of 0.62.

2.3. Benchmarking Data

We used the MTE global GPP data set (Jung et al., 2011) as a reference. It is a monthly global data product at 0.5° resolution which uses a statistical method based on machine learning techniques referred to as model tree ensembles (MTE). The MTE global GPP was trained against flux tower GPP estimates at site level using fAPAR from satellite observations and meteorological data as explanatory variables. Site level GPP estimates from 178 FLUXNET sites were incorporated in the production of the data following quality filtering and partitioning of net ecosystem exchange into GPP and ecosystem respiration based on Lasslop et al. (2010). The MTE product is available since 1982 but it is important to interpret it carefully since flux tower observations started a decade after that with a limited number of sites sparsely distributed and mainly across Europe and North America. Therefore, there is a large uncertainty of the MTE GPP over regions with limited flux tower sites including most parts of Africa and South America, as well as tropical and northern Asia (Anav et al., 2015).

3. Results

3.1. The Impact of Vegetation Canopy Structure on Modeled Global fAPAR

The first-order impact of adding clumping to the vegetation radiative transfer scheme in JULES is to reduce fAPAR. Figure 2 shows a global map of fAPAR differences between JULES with and without clumping

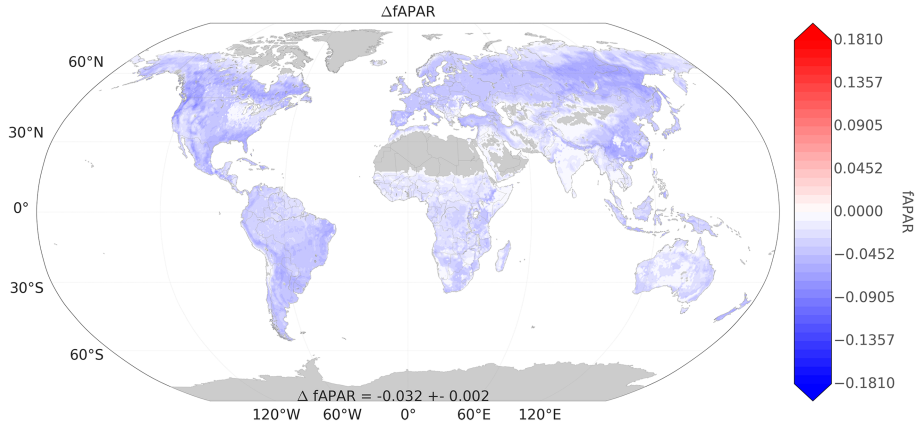

Figure 2. Spatial distribution of total fAPAR difference (JULES with clumping − JULES without clumping) for the year of 2008.

included. fAPAR decreases across the entire globe when clumping is added because it acts to decrease the effective leaf area available to intercept light. However, in addition to reducing the overall fAPAR, the relative distribution of absorption vertically through the canopy is also modified. Layers at the bottom canopy have more light directly incident upon them due to greater transmission through the layers above and therefore can potentially also absorb *more* PAR. Because clumping is applied to all layers evenly, each layer absorbs proportionally less of the PAR directly incident upon it, but the *total* amount of incident PAR on layers except for the top one will always be increased relative to the model without clumping. Hence, the total absorption of PAR in a layer can increase even though its fAPAR decreases as long as there is sufficient additional radiation reaching it.

The average value of fAPAR for the globe in 2008 according to JULES without clumping is 0.607 ± 0.022 (95% confidence interval). Applying the clumping index shifts the average value to 0.576 ± 0.021, or the equivalent of a total average decrease of 0.032 ± 0.002 (−5.3%). Some locations of the Earth have much larger divergences in fAPAR, for instance, Southwest Canada and Northwest USA, Northeast Russia, and high-altitude regions such as the Himalayas and the Andes; these are areas typically associated with needle-leaved trees.

3.2. The Impact of Vegetation Canopy Structure on Global GPP

In our model experiment the addition of clumping systematically *increases* carbon assimilation throughout the globe, resulting in an additional 5.53 ± 1.02 PgC/year in GPP. Figure 3 shows the difference in GPP

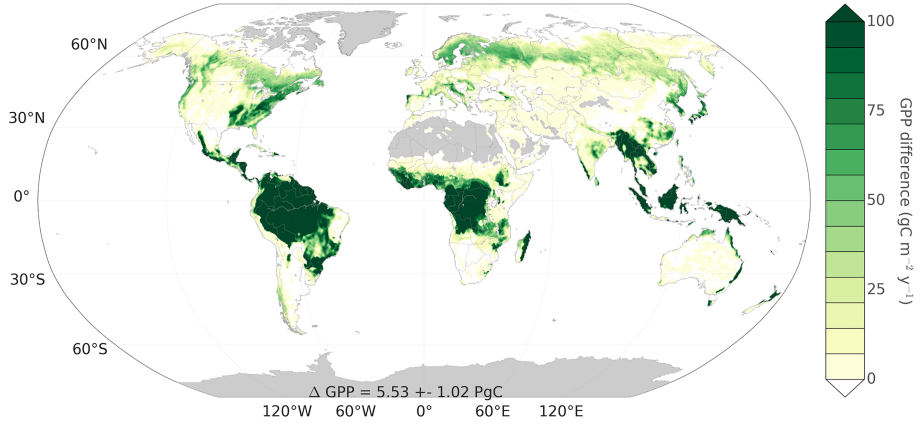

Figure 3. Difference in GPP between JULES with clumping and JULES without clumping. Global average values are indicated at the bottom of the figures in PgC/yr with the 95% confidence interval. Grey areas represent regions with no data.

between JULES with clumping (JULES-Clump) and the default version of JULES (i.e., without clumping). The strongest difference between the two model setups is found in the tropics (20°S–20°N) with additional GPP of 4.18 PgC/year, or 75% of the total additional carbon, followed by 1.10 PgC/year, or approximately 20% of the total extra GPP in the Northern Hemisphere (20°N–90°N), and 0.25 PgC/year in the Southern Hemisphere (90°S–20°S), which corresponds to approximately 5% of the total extra GPP.

Figure 4a shows the difference in the absolute difference between JULES-Clump and MTE-GPP, and JULES and MTE-GPP. Regions in blue indicate that including clumping moves the JULES prediction toward the MTE estimate, and red areas indicate the opposite; that is, JULES-Clump presents larger discrepancies than JULES in comparison to the MTE-GPP product. Tropical forests, the temperate forests in North America, and most of the boreal forests generally move closer the MTE data in JULES-Clump. The red areas on Figure 4a, associated with increasing differences between the MTE and modeled GPP prediction when clumping is included, are mainly found in the African and Brazilian savannahs, and sparser areas in the presence of grasses, especially C4 grasses. C4 grasses have previously been shown to be overproductive in JULES (Harper et al., 2016) and adding clumping makes it more productive in this study. It is also likely that the MTE data set itself shows an inaccurate representation of GPP for C4 grasses, since this PFT is not well sampled in the eddy covariance data that the MTE data set is based upon.

Figure 4c shows the total GPP in PgC/year for each box in Figure 4b for the MTE-GPP product, JULES and JULES-Clump, respectively. The error bars on the MTE product were calculated as the weighted sum of the averaged standard deviation of the ensemble mean of the 25 best model trees associated with the MTE-GPP product for the year 2008. JULES-Clump consistently shows a higher GPP than the default JULES for all the evaluated areas with a larger absolute impact over the boxes in the tropics, that is, Central and South America, $\Delta GPP = 2.03$ PgC/year, or 36.7% of the total additional GPP generated by the addition of clumping, followed by Africa, $\Delta GPP = 1.10$ PgC/year, or 19.9% of the total additional GPP, and South and Southeast Asia, $\Delta GPP = 1.05$ PgC/year, or 19.0% of the total additional GPP. Alone, the tropics are responsible for an extra 4.18 PgC per year (75.6% of the global ΔGPP).

Globally, the 5.53 PgC/year caused by the inclusion of vegetation clumping is equivalent to an additional 4.8% of GPP for the year of 2008. Although for the majority of regions in Figure 4b JULES GPP are within the error bars of the MTE product, JULES-Clump is closer to the estimates of the MTE, except for Africa, where JULES is lower than the MTE GPP and JULES-Clump is higher than it. The most significant change is observed over Central and South America where the prediction of GPP without clumping is low compared to the MTE GPP.

The additional GPP resulting from including clumping is not evenly distributed vertically though the canopy. The difference in zonal mean GPP in each canopy layer between JULES with and without clumping is shown in Figure 5. In particular there is a strong enhancement of GPP in the lower canopy layers for the tropics, whereas the top three or four layers exhibit reduced photosynthesis. This is caused by the increase in PAR absorption in the lower layers described in section 3.1. Because these layers tend to be light limited this results in a significant boost to the overall canopy photosynthesis compared to the upper layers which are generally not light limited (Alton et al., 2007; Huntingford et al., 2008; Jogireddy et al., 2006; Mercado et al., 2007). For the bottom two layers of the canopy GPP increased more than 50% throughout all latitudes. This adds further weight to the arguments of He et al. (2018) who highlight the importance of shade leaves in global photosynthesis.

3.3. Is the Impact of Vegetation Canopy Structure on Global GPP Impacted by Diffuse Radiation?

Throughout all simulations performed in this study the percentage of diffuse incident shortwave radiation was held constant and equal to 40% as a proxy average value for the whole globe (Harper et al., 2016). However, the consideration of gaps through the addition of clumping into the radiative transfer scheme in JULES can enhance the amount of shortwave radiation reaching bottom layers of the vegetation canopy, as previously discussed. This is true for both natures of incident light, that is, either direct, collimated beams, or diffuse, isotropic shortwave radiation. However, is the impact of canopy clumping on GPP affected by the amount of diffuse radiation?

In order to verify the effect of diffuse light on the impact of clumping on GPP, a test was performed for 12 FLUXNET sites for the year of 2008 with JULES and JULES-Clump for four different ratios of incident

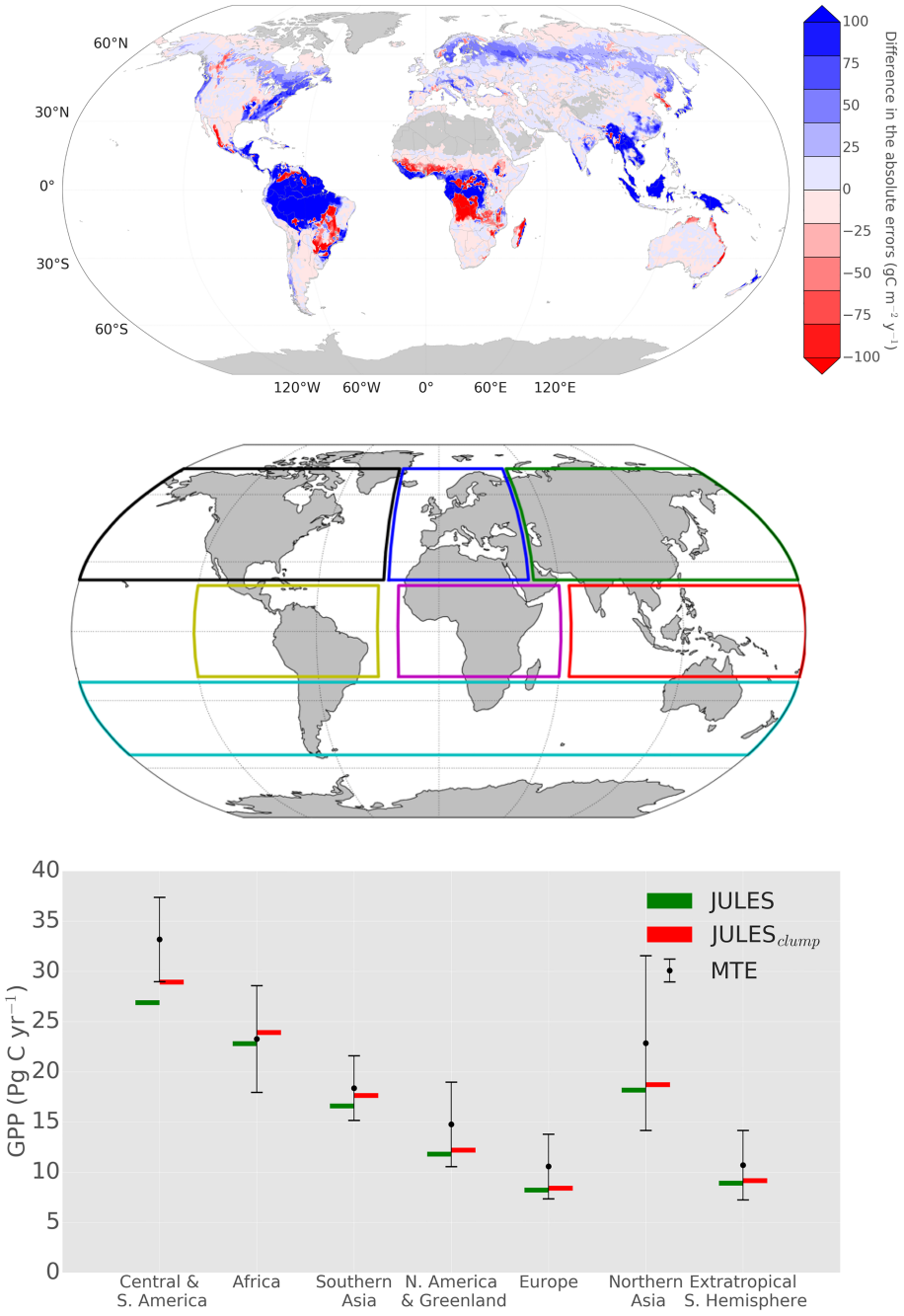

Figure 4. (a) The difference in the absolute GPP between JULES without clumping and the MTE data, and JULES with clumping and the MTE data. Regions in blue indicate model improvement by addition of vegetation clumping. (b) Map showing the regions used in the analysis. (c) Total (area weighted sum over box area) JULES (green), JULES-Clump (green), and observation based (MTE; black dots and error bars) GPP fluxes for the year of 2008 at regional scales. Error bars indicate the weighted sum of the averaged standard deviation of the ensemble mean of the 25 best model trees associated with the MTE-GPP product.

diffuse shortwave radiation to global incident shortwave radiation: 20%, 40% (used in all the other runs), 60%, and 80% (Figure 6). Results indicate that across all the evaluated sites, differences in monthly mean GPP fluxes between JULES and JULES-Clump are independent of the amount of diffuse shortwave radiation reaching the surface.

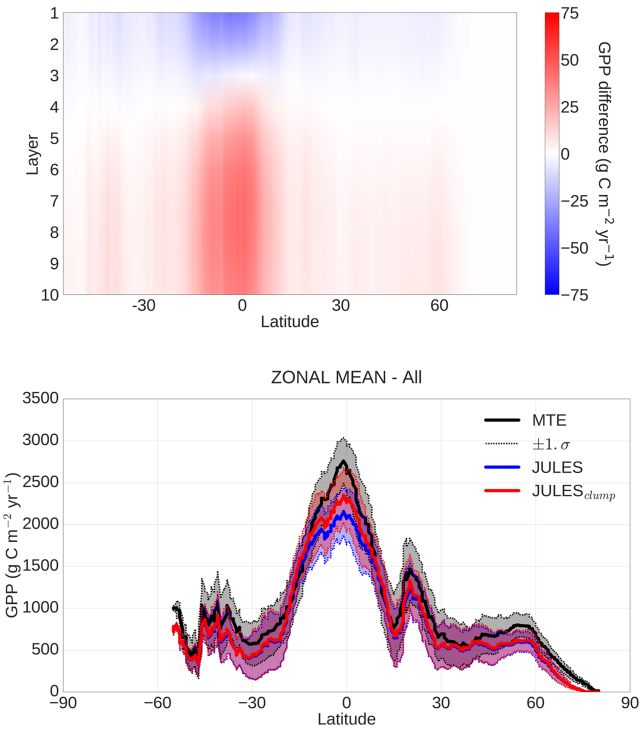

Figure 5. Zonal mean vertical profile of (a) absolute and difference in GPP between JULES-Clump and JULES without clumping. (b) Total GPP zonal mean of MTE, JULES-Clump (red), and JULES (blue). The 1 standard deviation ($\pm 1\sigma$) of the spatial mean for each product is represented by the filled areas.

One observable pattern in Figure 6 is the diffuse fertilization effect (Mercado et al., 2009) clearly noticed in sites with high LAI values, that is, the tropics (BR-Ma2, BR-Sa1) throughout the year, temperate forests (JP-Tak, US-MMS, US-Ha1), and boreal/needle-leaved forests (FI-Hyy, FI-Kaa, DE-Tha) in summer time, while places with smaller or no noticeable differences between JULES and JULES-Clump are noticed in sites that are not limited by light, because of small LAI values, often associated with drier/grassland sites (ES-Es1, ES-LMa, US-FPe).

4. Discussion

The only other study of which we are aware that tackles this question on a global scale is that of Chen et al. (2012). In that study the authors used a related data set to prescribe clumping in the Boreal Productivity Simulator (BEPS; Liu et al., 1997) but found that global GPP was *reduced* by 12.1 PgC/yr. The critical difference between our study and that of Chen et al. (2012) is in the treatment of canopy radiative transfer: our model uses multiple canopy layers each with different proportions of sunlit and shaded leaves, whereas Chen et al. (2012) use a single-layer split into sunlit and shaded leaves (a so-called "two-leaf" model). As discussed in the previous sections our result is caused by the greater penetration of light into lower layers boosting photosynthesis in layers that are light-limited. The phenomena we illustrate is to some degree analogous to the so-called "diffuse light fertilization effect" which has been shown previously to enhance global GPP after the eruption of Mount Pinatubo in 1991 (Mercado et al., 2009). Diffuse light is able to penetrate further down into the canopy than direct beam irradiance.

Single-layer models cannot redistribute absorbed radiation vertically in the manner we have shown using a layered canopy model. Consequently, there is no preferential alleviation of light-limited photosynthesis at lower levels and no boost to overall canopy photosynthesis. Other examples of models with multilayered canopy schemes include EALCO (Wang et al., 2001), EDv2.1 (Medvigy et al., 2009), LPJ-GUESS (Smith et al., 2001; Smith et al., 2014), SDGVM (Woodward et al., 1995), and TECO (Wang & Houlton, 2009), and so, similar results would be expected from these models assuming that the model structure allows for the inclusion of clumping in the canopy radiation scheme.

There is some empirical evidence from field-based studies that supports our finding that structure increases GPP (Ahl et al., 2004; Bohn & Huth, 2017; Duursma & Makela, 2007; Hardiman et al., 2011). Hardiman et al. (2011) showed departures from randomness in forest canopies boosted productivity in a transition zone between boreal forests and Northern mixed hardwood. The authors suggested that changes in canopy structure can contribute to resilience of the functioning of ecosystems trees. Atkins et al. (2018) affirm that the inclusion of canopy structural complexity metrics in canopy light absorption models could increase confidence in predictions of biogeochemical cycles and energy balance. Their study including sites from the National Ecological Observation Network and university field stations found that canopy structure was strongly coupled with fAPAR under high-light environments, while under low-light conditions, when diffuse light predominates, light scattering weakened the dependency of fAPAR on structure. Also, the authors found that a multivariate model including parameters of canopy structure and leaf area index explained around 89% of the intersite variance in fAPAR. Another observational study by Fahey et al. (2016) found an important contribution of bottom layers of a North American site to canopy productivity as whole. The authors found a connection between subcanopy tree growth and fAPAR, and indicated a relationship between subcanopy light availability and canopy structure. Although, they found that subcanopy growth response was not mediated by fAPAR alone.

On a global scale it will be necessary to provide observation of canopy structure from remote sensing instruments. The method of He et al. (2012) can, potentially, be repeated for every year of the MODIS archive and

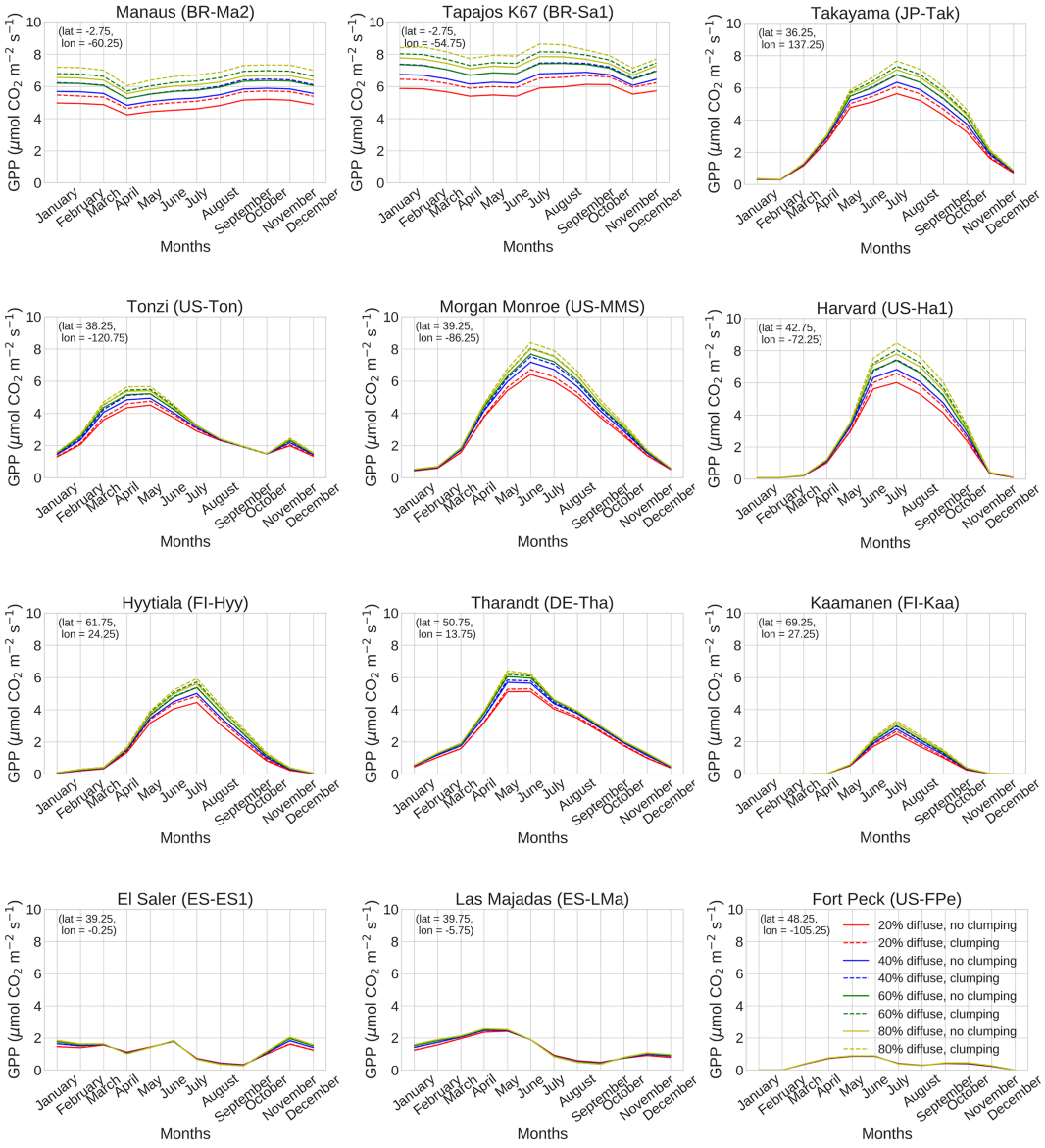

Figure 6. Monthly mean fluxes of GPP for 12 FLUXNET sites from JULES (continuous line) and JULES-Clump (dashed line) for four different percentages of incident diffuse shortwave radiation: 20% (red), 40% (blue), 60% (green), and 80% (yellow).

is applicable to other missions with similar characteristics such as Sentinel-3. Arguably, however, this problem also needs addressing using observations that are more directly related to forest structure such as space borne LiDAR from missions such as NASA GEDI (Hancock et al., 2019), or long-wavelength RADAR from JAXA's ALOS PALSAR the upcoming ESA Biomass mission. Terrestrial and airborne observations will also be critically important (Ferraz et al., 2018; Longo et al., 2016; Rödig et al., 2018) and the increased interest in terrestrial scanning LiDAR may help to answer some of these questions (Disney et al., 2010; Mulatu et al., 2019).

Our result that tropical photosynthesis is being underestimated in JULES likely applies to the terrestrial biosphere components of all ESMs. Multilayered models will respond in the same way when clumping is introduced, that is, with greater penetration of light to lower levels. We also argue that single-layer models do not represent the impact of clumping of photosynthesis correctly. It is clear, however, that much more investigation is required to understand the correct way to represent structure in these models. The technique used in JULES to include clumping is relatively simple albeit based on well-established theoretical considerations

(e.g., Nilson, 1971). We note that there are more sophisticated approaches available (Kucharik et al., 1999; Pinty et al., 2006; Ni-Meisters et al., 2010) but these rely on additional parameters which must either be calculated by the underlying land surface model, or input as ancillary data.

5. Conclusion

Our work suggests that ESMs may significantly underestimate global photosynthesis, especially in tropical forests, because they do not take vegetation structure into account. The dominant effect that introducing clumping has in our study is to alleviate light limitation at lower canopy levels. This tends to have the greatest impact where leaf area index is high and where photosynthesis is not limited by light in higher canopy layers. In our study this effect accounted for an additional uptake of carbon by photosynthesis globally of 5.53 and 4.18 PgC/year between 20°S and 20°N latitude.

Acknowledgments
The authors declare no conflicts of interest. This research was supported by the "Science without Borders" program (grant 9549-13-7) financed by CAPES–Brazilian Federal Agency for Support and Evaluation of Graduate Education within the Ministry of Education of Brazil. This research was carried out in part at INRA, Montpellier, France, where R.K. Braghiere was sponsored by the European Union's *Horizon 2020 Research and Innovation programme under grant agreement* 727217. This research was carried out in part at the Jet Propulsion Laboratory, California Institute of Technology, under a contract with the National Aeronautics and Space Administration. California Institute of Technology. Government sponsorship acknowledged. Support was provided in part by NASA's IDS program (PI Keenan, Co-I Fisher). Copyright 2019. All rights reserved. Tristan Quaife's contribution was funded by the NERC National Centre for Earth Observation (grant NE/R016518/1). The global clumping index map by He et al. (2012) is available for download through the following link: https://daac.ornl.gov/VEGETATION/guides/Global_Clumping_Index.html. The global clumping index map per PFT used in this study and a UNIX patch file for JULES version 4.6 is available from https://github.com/braghiere/JULES-Clump. The JULES code is available from the UK Met Office code repository: https://code.metoffice.gov.uk/. Model simulation results are available from https://doi.org/10.6084/m9.figshare.9727865.v1.We also thank M. Reichstein and M. Jung for providing MTE-GPP data through the site: https://www.bgc-jena.mpg.de/bgi/index.php/Services/Overview. The authors thank Pier Luigi Vidale, Sue Grimmond, Peter North, and the two anonymous reviewers, whose comments improved the manuscript.

References

Ahl, D. E., Gower, S. T., Mackay, D. S., Burrows, S. N., Norman, J. M., & Diak, G. R. (2004). Heterogeneity of light use efficiency in a northern Wisconsin forest: implications for modeling net primary production with remote sensing. *Remote Sensing of Environment*, *93*(1–2), 168–178. https://doi.org/10.1016/j.rse.2004.07.003

Alton, P., Mercado, L., & North, P. (2007). A sensitivity analysis of the land-surface scheme JULES conducted for three forest biomes: Biophysical parameters, model processes, and meteorological driving data. *Global Biogeochemical Cycles*, *21*, GB1008. https://doi.org/10.1029/2005GB002653

Anav, A., Friedlingstein, P., Beer, C., Ciais, P., Harper, A., Jones, C., et al. (2015). Spatiotemporal patterns of terrestrial gross primary production: A review. *Reviews of Geophysics*, *53*, 785–818. https://doi.org/10.1002/2015RG000483

Atkins, J. W., Fahey, R. T., Hardiman, B. H., & Gough, C. M. (2018). Forest Canopy Structural Complexity and Light Absorption Relationships at the Subcontinental Scale. *Journal of Geophysical Research: Biogeosciences*, *123*, 1387–1405. https://doi.org/10.1002/2017JG004256

Bartholomé, E., & Belward, A. S. (2005). GLC2000: A new approach to global land cover mapping from Earth observation data. *International Journal of Remote Sensing*, *26*(9), 1959–1977. https://doi.org/10.1080/01431160412331291297

Beer, C., Reichstein, M., Tomelleri, E., Ciais, P., Jung, M., Carvalhais, N., et al. (2010). Terrestrial Gross Carbon Dioxide Uptake: Global Distribution and Covariation with Climate. *Science*. https://doi.org/10.1126/science.1184984

Best, M. J., Pryor, M., Clark, D. B., Rooney, G. G., Essery, R. . L. H., Ménard, C. B., et al. (2011). The Joint UK Land Environment Simulator (JULES), model description. Part 1: Energy and water fluxes. *Geoscientific Model Development*, *4*(3), 677–699. Retrieved from http://nora.nerc.ac.uk/15031/, https://doi.org/10.5194/gmd-4-677-2011

Bohn, F. J., & Huth, A. (2017). The importance of forest structure to biodiversity–productivity relationships. *Royal Society Open Science*, *4*(1). https://doi.org/10.1098/rsos.160521

Chen, J. M., & Leblanc, S. G. (1997). A four-scale bidirectional reflectance model based on canopy architecture. *IEEE Transactions on Geoscience and Remote Sensing*, *35*, 1316–1337. https://doi.org/10.1109/36.628798

Chen, J. M., Menges, C. H., & Leblanc, S. G. (2005). Global derivation of the vegetation clumping index from multi-angular satellite data. *Remote Sensing of Environment*, *97*, 447–457. https://doi.org/10.1016/j.rse.2005.05.003

Chen, J. M., Mo, G., & Deng, F. (2017). A joint global carbon inversion system using both CO_2 and $^{13}CO_2$ atmospheric concentration data. *Geoscientific Model Development*, *10*(3), 1131–1156. https://doi.org/10.5194/gmd-10-1131-2017

Chen, J. M., Mo, G., Pisek, J., Liu, J., Deng, F., Ishizawa, M., & Chan, D. (2012). Effects of foliage clumping on the estimation of global terrestrial gross primary productivity. *Global Biogeochemical Cycles*, *26*, GB1019. https://doi.org/10.1029/2010GB003996

Ciais, P., Sabine, C., Bala, G., Bopp, L., Brovkin, V., Canadell, J., et al. (2013). Carbon and Other Biogeochemical Cycles. In T. F. Stocker, D. Qin, G.-K. Plattner, M. Tignor, S. K. Allen, J. Boschung, et al. (Eds.), *Climate Change 2013 - The Physical Science Basis, Contribution of Working Group I to the Fifth Assessment Report of the Intergovernmental Panel on Climate Change* (pp. 465–570). Cambridge, UK and New York, NY: Cambridge University Press.

Ciais, P., Tan, J., Wang, X., Roedenbeck, C., Chevallier, F., Piao, S.-L., et al. (2019). Five decades of northern land carbon uptake revealed by the interhemispheric CO_2 gradient. *Nature*, *568*(7751), 221–225. https://doi.org/10.1038/s41586-019-1078-6

Clark, D. B., & Gedney, N. (2008). Representing the effects of subgrid variability of soil moisture on runoff generation in a Land surface model. *Journal of Geophysical Research*, *113*, D10111. https://doi.org/10.1029/2007JD008940

Clark, D. B., Mercado, L. M., Sitch, S., Jones, C. D., Gedney, N., Best, M. J., et al. (2011). The Joint UK Land Environment Simulator (JULES), model description. Part 2: Carbon fluxes and vegetation dynamics. *Geoscientific Model Development*, *4*(3), 701–722. https://doi.org/10.5194/gmd-4-701-2011

Collatz, G. J., Ball, J. T., Grivet, C., & Berry, J. A. (1991). Physiological and environmental regulation of stomatal conductance, photosynthesis and transpiration: a model that includes a laminar boundary layer. *Agricultural and Forest Meteorology*, *54*(2–4), 107–136. https://doi.org/10.1016/0168-1923(91)90002-8

Collatz, G., Ribas-Carbo, M., & Berry, J. (1992). Coupled Photosynthesis-Stomatal Conductance Model for Leaves of C4 Plants. *Functional Plant Biology*, *19*(5), 519. https://doi.org/10.1071/PP9920519

Cox, P. M. (2001). Description of the " TRIFFID " Dynamic Global Vegetation Model. *Hadley Centre Technical Note*, *24*, 1–17.

Denman, K. L., Brasseur, G., Chidthaisong, A., Ciais, P., Cox, P. M., Dickinson, R. E., et al. (2007). Couplings Between Changes in the Climate System and Biogeochemistry. In S. Solomon, D. Qin, M. Manning, Z. Chen, M. Marquis, K. B. Averyt, et al. (Eds.), *Climate Change 2007: The Physical Science Basis. Contribution of Working Group I to the Fourth Assessment Report of the Intergovernmental Panel on Climate Change*. Cambridge, UK and New York, NY: Cambridge University Press.

Disney, M. I., Kalogirou, V., Lewis, P., Prieto-Blanco, A., Hancock, S., & Pfeifer, M. (2010). Simulating the impact of discrete-return lidar system and survey characteristics over young conifer and broadleaf forests. *Remote Sensing of Environment*, *114*(7), 1546–1560. https://doi.org/10.1016/j.rse.2010.02.009

Duursma, R. A., & Makela, A. (2007). Summary models for light interception and light-use efficiency of non-homogeneous canopies. *Tree Physiology*, *27*(6), 859–870. https://doi.org/10.1093/treephys/27.6.859

Fahey, R. T., Stuart-Haëntjens, E. J., Gough, C. M., De La Cruz, A., Stockton, E., Vogel, C. S., & Curtis, P. S. (2016). Evaluating forest subcanopy response to moderate severity disturbance and contribution to ecosystem-level productivity and resilience. *Forest Ecology and Management*, *376*, 135–147. https://doi.org/10.1016/j.foreco.2016.06.001

Farquhar, G. D., Caemmerer, S., & Berry, J. A. (1980). A biochemical model of photosynthetic CO_2 assimilation in leaves of C3 species. *Planta*, *149*(1), 78–90. https://doi.org/10.1007/BF00386231

Ferraz, A., Saatchi, S., Xu, L., Hagen, S., Chave, J., Yu, Y., et al. (2018). Carbon storage potential in degraded forests of Kalimantan, Indonesia. *Environmental Research Letters*, *13*(9). https://doi.org/10.1088/1748-9326/aad782

Hancock, S., Armston, J., Hofton, M., Sun, X., Tang, H., Duncanson, L. I., et al. (2019). The GEDI simulator: A large-footprint waveform lidar simulator for calibration and validation of spaceborne missions. *Earth and Space Science*. https://doi.org/10.1029/2018EA000506

Hardiman, B. S., Bohrer, G., Gough, C. M., Vogel, C. S., & Curtis, P. S. (2011). The role of canopy structural complexity in wood net primary production of a maturing northern deciduous forest. *Ecology*, *92*(9), 1818–1827. https://doi.org/10.1890/10-2192.1

Harper, A. B., Cox, P. M., Friedlingstein, P., Wiltshire, A. J., Jones, C. D., Sitch, S., et al. (2016). Improved representation of plant functional types and physiology in the Joint UK Land Environment Simulator (JULES v4.2) using plant trait information. *Geoscientific Model Development*, *9*(7), 2415–2440. https://doi.org/10.5194/gmd-9-2415-2016

He, L., Chen, J. M., Croft, H., Gonsamo, A., Luo, X., Liu, J., et al. (2017). Nitrogen Availability Dampens the Positive Impacts of CO_2 Fertilization on Terrestrial Ecosystem Carbon and Water Cycles. *Geophysical Research Letters*, *44*, 11,590–11,600. https://doi.org/10.1002/2017GL075981

He, L., Chen, J. M., Gonsamo, A., Luo, X., Wang, R., Liu, Y., & Liu, R. (2018). Changes in the Shadow: The Shifting Role of Shaded Leaves in Global Carbon and Water Cycles Under Climate Change. *Geophysical Research Letters*, *45*, 5052–5061. https://doi.org/10.1029/2018GL077560

He, L., Chen, J. M., Liu, J., Bélair, S., & Luo, X. (2017). Assessment of SMAP soil moisture for global simulation of gross primary production. *Journal of Geophysical Research: Biogeosciences*, *122*, 1549–1563. https://doi.org/10.1002/2016JG003603

He, L., Chen, J. M., Pisek, J., Schaaf, C. B., & Strahler, A. H. (2012). Global clumping index map derived from the MODIS BRDF product. *Remote Sensing of Environment*, *119*, 118–130.

He, L., Liu, J., Chen, J. M., Croft, H., Wang, R., Sprintsin, M., et al. (2016). Inter- and intra-annual variations of clumping index derived from the MODIS BRDF product. *International Journal of Applied Earth Observation and Geoinformation*, *44*, 53–60. https://doi.org/10.1016/j.jag.2015.07.007

Hogan, R. J., Quaife, T., & Braghiere, R. (2018). Fast matrix treatment of 3-D radiative transfer in vegetation canopies: SPARTACUS-Vegetation 1.1. *Geoscientific Model Development*, *11*(1), 339–350. https://doi.org/10.5194/gmd-11-339-2018

Huntingford, C., Fisher, R. A., Mercado, L., Booth, B. B. B., Sitch, S., Harris, P. P., et al. (2008). Towards quantifying uncertainty in predictions of Amazon "dieback". *Philosophical Transactions of the Royal Society of London. Series B, Biological Sciences*, *363*(1498), 1857–1864. https://doi.org/10.1098/rstb.2007.0028

Jiang, C., & Ryu, Y. (2016). Multi-scale evaluation of global gross primary productivity and evapotranspiration products derived from Breathing Earth System Simulator (BESS). *Remote Sensing of Environment*, *186*, 528–547. https://doi.org/10.1016/j.rse.2016.08.030

Jogireddy, V., Cox, P. M., Huntingford, C., Harding, R. J., & Mercado, L. M. (2006). *An improved description of canopy light interception for use in a GCM land-surface scheme: calibration and testing against carbon fluxes at a coniferous forest*. Exeter, UK: Met Office.

Jung, M., Reichstein, M., Margolis, H. A., Cescatti, A., Richardson, A. D., Arain, M. A., et al. (2011). Global patterns of land-atmosphere fluxes of carbon dioxide, latent heat, and sensible heat derived from eddy covariance, satellite, and meteorological observations. *Journal of Geophysical Research*, *116*, G00J07. https://doi.org/10.1029/2010JG001566

Knauer, J., Zaehle, S., Reichstein, M., Medlyn, B. E., Forkel, M., Hagemann, S., & Werner, C. (2017). The response of ecosystem water-use efficiency to rising atmospheric CO2concentrations: sensitivity and large-scale biogeochemical implications. *New Phytologist*, *213*(4), 1654–1666. https://doi.org/10.1111/nph.14288

Kobayashi, H., Baldocchi, D. D., Ryu, Y., Chen, Q., Ma, S., Osuna, J. L., & Ustin, S. L. (2012). Modeling energy and carbon fluxes in a heterogeneous oak woodland: A three-dimensional approach. *Agricultural and Forest Meteorology*, *152*(1), 83–100.

Koffi, E. N., Rayner, P. J., Scholze, M., & Beer, C. (2012). Atmospheric constraints on gross primary productivity and net ecosystem productivity: Results from a carbon-cycle data assimilation system. *Global Biogeochemical Cycles*, *26*, GB1024. https://doi.org/10.1029/2010GB003900

Kucharik, C. J., Norman, J. M., & Gower, S. T. (1999). Characterization of radiation regimes in nonrandom forest canopies: theory, measurements, and a simplified modeling approach. *Tree Physiology*, *19*(11), 695–706.

Lasslop, G., Reichstein, M., Papale, D., Richardson, A., Arneth, A., Barr, A., et al. (2010). Separation of net ecosystem exchange into assimilation and respiration using a light response curve approach: Critical issues and global evaluation. *Global Change Biology*, *16*(1), 187–208. https://doi.org/10.1111/j.1365-2486.2009.02041.x

le Quéré, C., Andrew, R. M., Friedlingstein, P., Sitch, S., Hauck, J., Pongratz, J., et al. (2018). Global Carbon Budget 2018. *Earth System Science Data*, *10*(4), 2141–2194. https://doi.org/10.5194/essd-10-2141-2018

le Quéré, C., Andrew, R. M., Friedlingstein, P., Sitch, S., Pongratz, J., Manning, A. C., et al. (2018). Global Carbon Budget 2017. *Earth System Science Data*, *10*(1), 405–448. https://doi.org/10.5194/essd-10-405-2018

Liu, J., Chen, J. M., Cihlar, J., & Park, W. M. (1997). A process-based boreal ecosystem productivity simulator using remote sensing inputs. *Remote Sensing of Environment*, *62*(2), 158–175. https://doi.org/10.1016/S0034-4257(97)00089-8

Loew, A., Van Bodegom, P. M., Widlowski, J. L., Otto, J., Quaife, T., Pinty, B., & Raddatz, T. (2014). Do we (need to) care about canopy radiation schemes in DGVMs? Caveats and potential impacts. *Biogeosciences*, *11*(7), 1873–1897.

Longo, M., Keller, M., dos-Santos, M. N., Leitold, V., Pinagé, E. R., Baccini, A., et al. (2016). Aboveground biomass variability across intact and degraded forests in the Brazilian Amazon. *Global Biogeochemical Cycles*, *30*, 1639–1660. https://doi.org/10.1002/2016GB005465

MacBean, N., Maignan, F., Bacour, C., Lewis, P., Peylin, P., Guanter, L., et al. (2018). Strong constraint on modelled global carbon uptake using solar-induced chlorophyll fluorescence data. *Scientific Reports*, *8*(1), 1973. https://doi.org/10.1038/s41598-018-20024-w

Medvigy, D., Wofsy, S. C., Munger, J. W., Hollinger, D. Y., & Moorcroft, P. R. (2009). Mechanistic scaling of ecosystem function and dynamics in space and time: Ecosystem Demography model version 2. *Journal of Geophysical Research*, *114*, G01002. https://doi.org/10.1029/2008JG000812

Melillo, J., Prentice, I., Farquhar, G., & Leemans, R. (1995). Terrestrial biotic responses to environmental change and feedbacks to climate. In J. Houghton, L. Meira Filho, & B. Callander (Eds.), *Climate change 1995: the science of climate change* (pp. 447–481). Cambridge, England: Cambridge University Press.

Mercado, L. M., Bellouin, N., Sitch, S., Boucher, O., Huntingford, C., Wild, M., & Cox, P. M. (2009). Impact of changes in diffuse radiation on the global land carbon sink. *Nature*, *458*(7241), 1014–1017. https://doi.org/10.1038/nature07949

Mercado, L. M., Huntingford, C., Gash, J. H. C., Cox, P. M., & Jogireddy, V. (2007). Improving the representation of radiation interception and photosynthesis for climate model applications. *Tellus, Series B: Chemical and Physical Meteorology*, *59*(3), 553–565. https://doi.org/10.1111/j.1600-0889.2007.00256.x

Mulatu, K., Decuyper, M., Brede, B., Kooistra, L., Reiche, J., Mora, B., & Herold, M. (2019). Linking Terrestrial LiDAR Scanner and Conventional Forest Structure Measurements with Multi-Modal Satellite Data. *Forests*, *10*(3), 291. https://doi.org/10.3390/f10030291

Nachtergaele, F., van Velthuizen, H., Verelst, L., Batjes, N., Dijkshoorn, K., van Engelen, V., et al. (2008). *Harmonized World Soil Database (version 1.0). Rome, Italy and IIASA, Laxenburg*. Austria: FAO.

Nilson, T. (1971). A theoretical analysis of the frequency of gaps in plant stands. *Agricultural Meteorology*, *8*, 25–38. https://doi.org/10.1016/0002-1571(71)90092-6

Ni-Meister, W., Yang, W., & Kiang, N. Y. (2010). A clumped-foliage canopy radiative transfer model for a global dynamic terrestrial ecosystem model I: Theory. *Agricultural and Forest Meteorology*, *150*(7–8), 881–894. https://doi.org/10.1016/j.agrformet.2010.02.009

Olivas, P. C., Oberbauer, S. F., Clark, D. B., Clark, D. A., Ryan, M. G., O'Brien, J. J., & Ordoñez, H. (2013). Comparison of direct and indirect methods for assessing leaf area index across a tropical rain forest landscape. *Agricultural and Forest Meteorology*, *177*, 110–116. https://doi.org/10.1016/j.agrformet.2013.04.010

Pinty, B., Lavergne, T., Dickinson, R. E., Widlowski, J. L., Gobron, N., & Verstraete, M. M. (2006). Simplifying the interaction of land surfaces with radiation for relating remote sensing products to climate models. *Journal of Geophysical Research*, *111*, D02116. https://doi.org/10.1029/2005JD005952

Pisek, J., & Oliphant, A. J. (2013). A note on the height variation of foliage clumping: comparison with remote sensing retrievals. *Remote Sensing Letters*, *4*(4), 400–408. https://doi.org/10.1080/2150704X.2012.742212

Prentice, I. C., Farquhar, G. D., Fasham, M. J. R., Goulden, M. L., Heimann, M., Jaramillo, J. V, et al. (2001). The carbon cycle and atmospheric carbon dioxide. In J. T. Houghton, Y. Ding, D. J. Griggs, M. Noguer, P. J. van der Linden, X. Dai, et al. (Eds.), *Climate change 2001: the scientific basis* (pp. 183–237). Cambridge University Press.

Rödig, E., Cuntz, M., Rammig, A., Fischer, R., Taubert, F., & Huth, A. (2018). The importance of forest structure for carbon fluxes of the Amazon rainforest. *Environmental Research Letters*, *13*(5). https://doi.org/10.1088/1748-9326/aabc61

Ross, J. (1981). *The radiation regime and architecture of plant stands*. Boston: Junk. https://doi.org/10.1007/978-94-009-8647-3

Sellers, P. J. (1985). Canopy reflectance, photosynthesis and transpiration. *International Journal of Remote Sensing*, *6*(8), 1335–1372. https://doi.org/10.1080/01431168508948283

Smith, B., Prentice, I. C., & Sykes, M. T. (2001). Representation of vegetation dynamics in the modelling of terrestrial ecosystems: Comparing two contrasting approaches within European climate space. *Global Ecology and Biogeography*, *10*(6), 621–637. https://doi.org/10.1046/j.1466-822X.2001.00256.x

Smith, B., Wärlind, D., Arneth, A., Hickler, T., Leadley, P., Siltberg, J., & Zaehle, S. (2014). Implications of incorporating N cycling and N limitations on primary production in an individual-based dynamic vegetation model. *Biogeosciences*, *11*(7), 2027–2054. https://doi.org/10.5194/bg-11-2027-2014

Walters, D. N., Williams, K. D., Boutle, I. A., Bushell, A. C., Edwards, J. M., Field, P. R., et al. (2014). The Met Office Unified Model Global Atmosphere 4.0 and JULES Global Land 4.0 configurations. *Geoscientific Model Development*, *7*(1), 361–386. https://doi.org/10.5194/gmd-7-361-2014

Wang, S., Grant, R. F., Verseghy, D. L., & Black, T. A. (2001). Modelling plant carbon and nitrogen dynamics of a boreal aspen forest in CLASS - The Canadian Land Surface Scheme. *Ecological Modelling.*, *142*(1-2), 135–154. https://doi.org/10.1016/S0304-3800(01)00284-8

Wang, Y. P., & Houlton, B. Z. (2009). Nitrogen constraints on terrestrial carbon uptake: Implications for the global carbon-climate feedback. *Geophysical Research Letters*, *36*, L24403. https://doi.org/10.1029/2009GL041009

Watson, R. T., Rohde, H., Oeschger, H., & Siegenthaler, U. (1990). Greenhouse gases and aerosols. In J. T. Houghton, B. A. Callandar, & S. K. Varney (Eds.), *Climate change: the IPCC scientific assessment* (pp. 7–40). Cambridge, England: Cambridge University Press.

Weedon, G. P., Balsamo, G., Bellouin, N., Gomes, S., Best, M. J., & Viterbo, P. (2014). The WFDEI meteorological forcing data set: WATCH Forcing data methodology applied to ERA-Interim reanalysis data. *Water Resources Research*, *50*, 7505–7514. https://doi.org/10.1002/2014WR015638

Welp, L. R., Keeling, R. F., Meijer, H. A. J., Bollenbacher, A. F., Piper, S. C., Yoshimura, K., et al. (2011). Interannual variability in the oxygen isotopes of atmospheric CO_2 driven by El Niño. *Nature*, *477*(7366), 579–582. https://doi.org/10.1038/nature10421

Williams, K., Gornall, J., Harper, A., Wiltshire, A., Hemming, D., Quaife, T., et al. (2017). Evaluation of JULES-crop performance against site observations of irrigated maize from Mead, Nebraska. *Geoscientific Model Development*, *10*(3), 1291–1320. https://doi.org/10.5194/gmd-10-1291-2017

Woodward, F. I., Smith, T. M., & Emanuel, W. R. (1995). A global land primary productivity and phytogeography model. *Global Biogeochemical Cycles*, *9*(4), 471–490. https://doi.org/10.1029/95GB02432

Yang, R., Friedl, M. A., & Ni, W. (2001). Parameterization of shortwave radiation fluxes for nonuniform vegetation canopies in land surface models. *Journal of Geophysical Research*, *106*(D13). https://doi.org/10.1029/2001JD900180